Journal of Cellular Biochemistry 93:1272–1281 (2004)

Unique Precipitation and Exocytosis of a Calcium Salt of *myo*-Inositol Hexakisphosphate in Larval *Echinococcus granulosus*

Florencia Irigoín,[1] Cecilia Casaravilla,[1] Francisco Iborra,[2] Robert B. Sim,[3] Fernando Ferreira,[4] and Alvaro Díaz[1]*

[1]Cátedra de Inmunología, Facultad de Química/Ciencias, Universidad de la República, Uruguay
[2]MRC Molecular Haematology Unit, The Weatherall Institute of Molecular Medicine, University of Oxford, United Kingdom
[3]MRC Immunochemistry Unit, Department of Biochemistry, University of Oxford, United Kingdom
[4]Laboratorio de Carbohidratos y Glicoconjugados, Facultad de Química/Medicina, Universidad de la República, Uruguay

Abstract The ubiquitous intracellular molecule *myo*-inositol hexakisphosphate (IP_6) is present extracellularly in the hydatid cyst wall (HCW) of the parasitic cestode *Echinococcus granulosus*. This study shows that extracellular IP_6 is present as its solid calcium salt, in the form of deposits that are observed, at the ultrastructural level, as naturally electron dense granules some tens of nanometers in diameter. The presence of a calcium salt of IP_6 in these structures was determined by two different electron microscopy techniques: (i) the analysis of the spatial distribution of phosphorus and calcium in the outer, acellular layer of the HCW (the laminated layer, LL) through electron energy loss spectroscopy, and (ii) the observation, by transmission electron microscopy, of HCW that were selectively depleted of IP_6 by treatment with EGTA or phytase, an enzyme that catalyses the dephosphorylation of IP_6. The deposits of the IP_6-Ca(II) salt are also observed inside membrane vesicles in cells of the germinal layer (the inner, cellular layer of the HCW), indicating that IP_6 precipitates with calcium within a cellular vesicular compartment and is then secreted to the LL. Thus, much as in plants (that produce vesicular IP_6 deposits), the existence of transporters for IP_6 or its precursors in internal membranes is needed to explain the compound's cellular localisation in *E. granulosus*. J. Cell. Biochem. 93: 1272–1281, 2004.

Key words: calcium; phytic acid; inositol polyphosphates; cestode; hydatidosis

myo-Inositol hexakisphosphate (IP_6) is an ubiquitous intracellular molecule in eukaryotes, thought to have a cytosolic and nuclear distribution [Irvine and Schell, 2001; Shears, 2001; Raboy, 2003]. In a previous article, we reported that in the larva of the parasitic cestode *Echinococcus granulosus*, IP_6 is localised extracellularly [Irigoín et al., 2002]. This larva has the form of a fluid-filled cyst, limited by a two-layered structure named the hydatid cyst wall (HCW). The outer layer of the HCW, in direct contact with the host tissue, is the laminated layer (LL), an acellular meshwork composed mainly of glycoconjugates [Kilejian et al., 1962; Kilejian and Schwabe, 1971]. The LL, attaining up to 2 mm thickness, is a conspicuous structure found only in the members of the genus *Echinococcus*. It is synthesised by the underlying, cellular layer of the HCW, named germinal layer. The LL provides the cyst with mechanical support and protects the parasite cells from direct contact with the potentially

Abbreviations used: IP_6, *myo*-inositol hexakisphosphate; HCW, hydatid cyst wall; LL, laminated layer; PEI, polyethyleneimine; TCA, trichloroacetic acid; EELS, electron energy loss spectroscopy; TEM, transmission electron microscopy; ER, endoplasmic reticulum.

Florencia Irigoín's present address is Center for Free Radical and Biomedical Research, Departamento de Bioquímica, Facultad de Medicina, Universidad de la República, Uruguay.

*Correspondence to: Alvaro Díaz, Cátedra de Inmunología, Instituto de Higiene, Avda. Alfredo Navarro 3051, piso 2. CP 11600, Montevideo, Uruguay. E-mail: adiaz@fq.edu.uy

Received 2 April 2004; Accepted 4 June 2004

DOI 10.1002/jcb.20262

harmful host cells. It is in this unusual structure that we found the extracellular IP_6; in addition, smaller absolute amounts of IP_6 are present in the germinal layer, as fits a parasite-synthesised component [Irigoín et al., 2002]. IP_6 is a major component of the HCW, where it is immobilised by the interaction with Ca^{2+}. Indeed, we observed that the association with IP_6 would account for the majority of the Ca^{2+} present in the HCW [Irigoín et al., 2002], thus explaining the much higher abundance of this element in relation to Mg^{2+} [Sadanand, 1971]. These observations drew our attention to one of the ultrastructural elements previously described in the LL, namely, the so-called granular bodies: these have been determined to be rich in Ca^{2+} by X-ray microanalysis (mentioned in [Rogan and Richards, 1989]).

Electron micrographs of the *E. granulosus* HCW have consistently shown that the LL is formed by two ultrastructural elements: a predominant microfibrillar matrix and the granular bodies [Morseth, 1967; Bortoletti and Ferretti, 1978; Richards et al., 1983a; Rogan and Richards, 1989]. The microfibrillar matrix stains positive for carbohydrates, and is thus thought to be made up from the glycoconjugates that account for the bulk of the LL chemically [Richards et al., 1983a]. The granular element was described in detail by Richards et al. [1983a]: it consists of naturally electron-dense bodies of defined size (41 ± 1 nm in diameter) that are found irregularly dispersed, individually or in aggregates, among the fibres. Individual granules are also observed within vesicles in germinal layer cells, and seem to be exocytosed towards the LL. Whereas the microfibrillar matrix is a common feature of the LL of all *Echinococcus* species [Ingold et al., 2000, 2001], the granules have been described only in *E. granulosus*.

In the present work, we have established the ultrastructural localisation of IP_6 in the HCW by means of two different electron microscopy techniques. The results demonstrate that an insoluble IP_6-Ca(II) salt is the main component of the granular element of the *E. granulosus* LL.

MATERIALS AND METHODS

Materials

IP_6 (hexasodium salt), phytase from *Aspergillus ficuum* and general chemicals were purchased from Sigma (St. Louis, MO). Polyethyleneimine (PEI)-cellulose TLC plates were obtained from Macherey-Nagel (Düren, Germany).

E. granulosus Cysts

Bovine hydatid cysts from natural infections, and murine cysts from experimental infections were obtained as described previously [Irigoín et al., 2002]. The latter, measuring 0.2–1.0 cm in diameter, can be manipulated in toto; also, their thin (around 80 μm) LL allows efficient extraction of IP_6 by EDTA/EGTA treatment without previous homogenisation. In other experiments, murine or bovine HCW were pulverised: pooled material from several cysts was washed extensively with 2 M NaCl, 0.5 mM $CaCl_2$ followed by 0.5 mM $CaCl_2$, and then ground under mortar and pestle after dehydration in ethanol (95%) followed by acetone.

Dephosphorylation of IP_6 by Phytase

Phytase-catalysed IP_6 dephosphorylation was monitored as released orthophosphate, quantitated by its reaction with ammonium molybdate [Chen et al., 1956] using sodium phosphate as standard. In one type of experiment, dephosphorylation was employed to measure the IP_6 content of the HCW: pulverised HCW was incubated at 37°C with 0.75 U of phytase/mg of HCW dry mass in 0.2 M glycine/HCl buffer (pH 2.5). Reactions were stopped by addition of 7.5% (w/v) TCA; samples were then centrifuged, and phosphate quantitated in the supernatants. As a control, the calcium salt of IP_6 was treated in the same way; this salt was prepared and its stoichiometry determined by Carlos Kremer (Inorganic Chemistry Lab, Faculty of Chemistry, University of Uruguay, unpublished results). In other cases, enzymatic dephosphorylation was tested as a tool to remove IP_6 selectively from the HCW. For this purpose, pulverised HCW was incubated at 37°C with 0.75 U of phytase/mg of HCW dry mass in 200 mM sodium acetate/acetic acid buffer (pH 5.0), containing 100 mM $CaCl_2$, and intact murine cysts were incubated with 100 μl of 7.5 U/ml of phytase/cyst (0.2–0.4 cm in diameter) in the same buffer but containing 500 mM $CaCl_2$. Control reactions were carried out in which phytase was omitted. In order to evaluate the degree of dephosphorylation achieved, reactions were stopped by the addition of TCA, and phosphate was quantitated in the superna-

tants. For assessing the amount of IP_6 remaining in the HCW, the insoluble residue from the pulverised HCW, or the whole murine cysts, were extracted with 0.5 ml/mg of HCW initial dry mass or 1.2 ml/cyst of 100 mM Tris/HCl buffer (pH 7.35) containing 10 mM EDTA. The supernatants were extensively dialysed against distilled water and analysed for IP_6 by TLC on PEI plates as described previously [Spencer et al., 1990].

NMR Analyses

^{1}H-NMR spectra were recorded for solutions in ^2H_2O at 30°C using a Brücker Avance DPX 400 instrument (Acton, MA) at 400 MHz. ^{1}H chemical shifts were reported in ppm using 3-trimethyl-silyl propionate (δ_H 0.00) as internal reference.

Electron Energy Loss Spectroscopy (EELS)

Intact murine cysts were washed extensively with 20 mM Tris/HCl buffer (pH 7.0) containing 150 mM NaCl. The cyst fluid was aspirated and the HCW cut into small pieces that were fixed with 3% (w/v) glutaraldehyde in 100 mM sodium cacodylate buffer (pH 7.2) for 2 h at 4°C; samples were left in 1% (w/v) paraformaldehyde in the same buffer until further processing. Samples were dehydrated in graded ethanol series and embedded in Epon 812, following manufacturer instructions. Heavy metals were not used, since they interfere with EELS analysis. Twenty to forty nanometer sections were obtained with a diamond knife, collected on uncoated 700-mesh grids, and examined in a Leo 912 AB transmission electron microscope (Leo Electron Microscopy, UK) equipped with an integrated Omega energy filter. EELS micrographs were taken at 120, 130, and 155 eV for phosphorus determination; 300, 320, and 350 eV for calcium; 250, 275, and 300 eV for carbon; 500, 525, and 540 eV for oxygen and 350, 375, and 410 eV for nitrogen. An electron energy loss spectrum in the region corresponding to phosphorus was acquired for selected regions of the sample by obtaining images at intervals of 2 eV, from 124 to 176 eV, and plotting the intensity of the signals versus energy.

Transmission Electron Microscopy (TEM)

Murine HCW were fixed with 3% glutaraldehyde in 100 mM sodium cacodylate buffer (pH 7.2) with 0.5 mM $CaCl_2$ and 0.25% (w/v) tannic acid [Ingold et al., 2000], for 3 h at 4°C. Samples were dehydrated in graded ethanol series and embedded in araldite. Fifty nanometer sections were obtained with a glass knife and collected on Formvar and carbon coated grids (200 mesh). Grids were incubated with 20 μl of 100 mM Tris/HCl buffer (pH 7.4) containing 10 mM EGTA or 0.5 mM $CaCl_2$ as a control. Alternatively, they were incubated with 20 μl of a solution containing 15 U/ml of phytase in 200 mM sodium acetate/acetic acid buffer (pH 5.0) containing 100 mM $CaCl_2$, or the same buffer without enzyme as a control. In both cases, the incubations were performed at 37°C for 30 min. After treatment, grids were washed with 20 μl of 100 mM Tris/HCl (pH 7.35) containing 0.5 mM $CaCl_2$, then with 20 μl of deionised water and stained with saturated aqueous uranyl acetate followed by lead citrate. Electron micrographs were obtained by Gabriela Casanova and Alvaro Olivera (Transmission Electron Microscopy Facility, Faculty of Sciences, University of Uruguay) in a JEOL (JEM-1010) instrument, at 80 kV.

RESULTS

Calcium IP_6 Accounts for at Least one-Quarter of the HCW dry Mass

In our previous work, we had observed that IP_6 was extracted from the HCW only in the presence of EDTA. We also reported that upon EDTA treatment, Ca^{2+} co-solubilised with IP_6 in a ratio of 8 moles per mol of IP_6, whereas the corresponding figure for Mg^{2+} was less than unity; this suggested that IP_6 in the HCW was interacting with Ca^{2+} and not with Mg^{2+}. This notion was strengthened by the observation that similar amounts of IP_6 were extracted from intact murine cysts by EDTA or by EGTA, a chelating agent with much higher affinity for Ca^{2+} than Mg^{2+} (Fig. 1, third and fourth lanes). In addition, some IP_6 was solubilised even in the absence of chelating agents when large volumes of buffer were used, and this was prevented by including Ca^{2+} in the incubation buffer (Fig. 1, first and second lanes). Recent studies on the chemistry of IP_6 have shown that its calcium salt has the stoichiometry $Ca_5H_2IP_6 \cdot 16\ H_2O$, independently of the precipitation conditions employed (C. Kremer, Inorganic Chemistry Lab, Faculty of Chemistry, University of Uruguay, unpublished results). If, as it now seems likely, the IP_6 of the HCW is forming this same species, this would account for a smaller

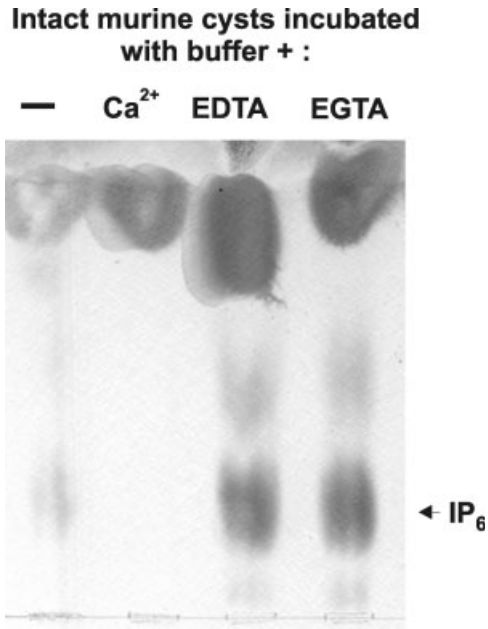

Fig. 1. IP_6 solubilisation from intact cysts by different buffers. Murine cysts were incubated for 3 h at 25°C with 0.3 ml per cyst (0.5–1 cm in diameter) of 20 mM Tris/HCl buffer (pH 7.0), alone or containing 5 mM $CaCl_2$, or 5 mM EDTA, or 5 mM EGTA. The supernatants were dialysed against distilled water and a fraction thereof (1/30) analysed by TLC on PEI-cellulose plates.

proportion of the HCW Ca^{2+} than previously calculated assuming a hexacalcium species (around 60 instead of 70%). The chemical studies mentioned also indicate that the calcium salt of IP_6 has a low but measurable solubility at neutral pH; being governed by a solubility product constant, this solubility is expected to decrease in the presence of excess soluble Ca^{2+}. While explaining the observations in Figure 1, these ideas also suggested that our previous estimations for the IP_6 content of the HCW would be affected by IP_6 losses during the initial wash of parasite material in buffers lacking Ca^{2+}.

The IP_6 content of the HCW was therefore reassessed in light of the better understanding of the relevant chemistry. Also, this time the estimation was based on the amount of orthophosphate released from the HCW after its digestion with phytase, an enzyme that dephosphorylates IP_6 to inositol monophosphates and inositol. The enzyme activity was first assayed on the calcium salt of IP_6: at pH 2.5 and 37°C orthophosphate release reached a plateau in half an hour (Fig. 2). This was observed for amounts of IP_6 (140–350 nmol) bracketing the ones later estimated for the HCW materials. Then, pulverised HCW from bovine and murine cysts were treated in the same way. As observed for the IP_6-Ca(II) salt, phosphate release was maximum after half an hour incubation (Fig. 2). The IP_6 content was estimated taking into account the degree of dephosphorylation achieved for pure calcium-IP_6 (80% the figure expected for stoichiometric hydrolysis to inositol): expressed in terms of $Ca_5H_2IP_6 \cdot 16H_2O$, it accounted for approximately a third and a

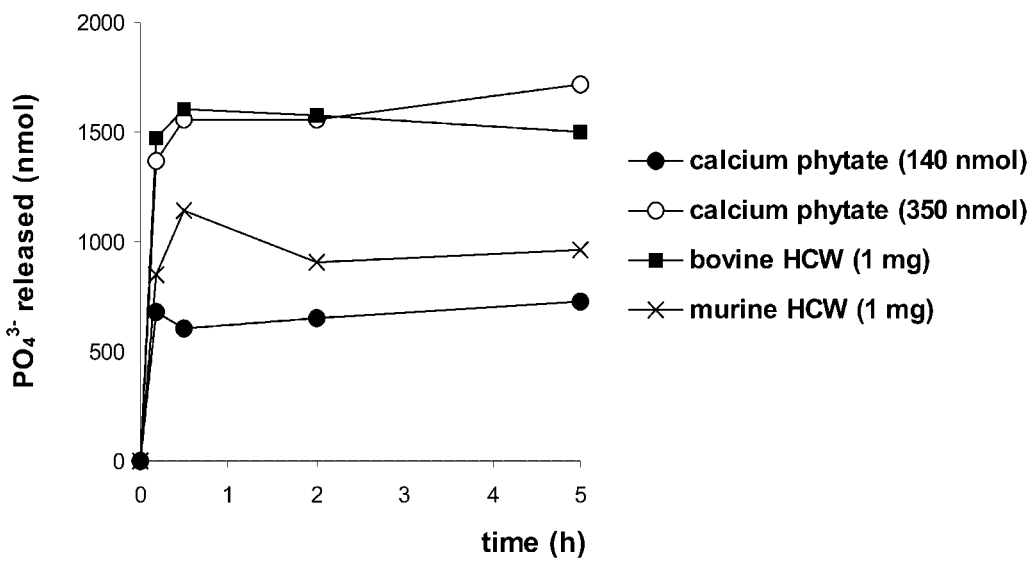

Fig. 2. Enzymatic dephosphorylation of IP_6 from pulverised HCW. One milligram (dry mass) of HCW samples or different amounts of the pure calcium-IP_6 salt were treated with phytase at pH 2.5 as described in Materials and Methods, and orthophosphate released was quantitated.

TABLE I. Estimation of the IP_6 Content of the HCW

	Bovine HCW	Murine HCW
Phytase released PO_4^{3-}/mass of HCW (nmol/mg)	1,600	1,000
IP_6/mass of HCW (μmol/g)	330	210
Mass of $Ca_5H_2IP_6 \cdot 16\ H_2O$/mass of HCW (%)	37	24
Total PO_4^{3-}/mass of HCW (μmol/g)	2,400	1,600
PO_4^{3-} in HCW as IP_6 (%)	82	79

IP_6 estimations are based on the amounts of orthophosphate released by phytase as shown in Figure 2. Values from time points after the reactions reached plateux (0.5, 2, and 5 h) were averaged and phosphate released in the absence of enzyme subtracted. IP_6 contents were then estimated taking into account the degree of dephosphorylation obtained for the pure IP_6-Ca(II) salt (80%). The proportion of the HCW dry mass accounted for by IP_6 is expressed in terms of the only known calcium salt of IP_6, which has the stoichiometry $Ca_5H_2IP_6 \cdot 16\ H_2O$. The total phosphorus content of the materials was estimated after acid digestion as described before [Irigoín et al., 2002].

quarter of the dry mass of bovine and murine HCW respectively (Table I). There is a logical reason for inclusion of crystallisation/coordination water in a calculation involving dry mass: such water molecules are part of a solid phase, and are not removed by usual drying methods applied to biological samples. The new estimations for IP_6 content are considerably higher than those obtained in our previous work (5 and 13% for bovine and murine cysts respectively, when expressed as $Ca_5H_2IP_6 \cdot 16H_2O$), in which the estimation was based on IP_6 extraction by EDTA, followed by its quantitation by TLC and densitometry. In addition to the IP_6 losses during washes mentioned above, the difference is explained by two factors, both mentioned in our previous work: (i) we had not verified that IP_6 extraction was complete, and (ii) although IP_6 can be desalted by dialysis [Van der Kaay and Van Haastert, 1995], this procedure applied to the extracts may have caused IP_6 losses.

Calcium-IP_6 Makes up the Previously Described Naturally Electron-Dense Granules of the LL

As we had previously stated, IP_6 accounted for the bulk of the total phosphorus of the HCW [Irigoín et al., 2002]; this was confirmed by measurements in this work (Table I). This observation opened the possibility of assessing the ultrastructural localisation of IP_6 in the LL through mapping the distribution of phosphorus by electron energy loss spectroscopy (EELS). In this technique, the specific energy loss of primary electrons when inelastically scattered by a given element is used to image the spatial distribution of the element in the sample with high resolution. The distribution of phosphorus, calcium, oxygen, carbon, and nitrogen was studied in the HCW from a murine cyst. Figure 3A,D show EELS images obtained at 0 eV, a condition corresponding to the conventional transmission electron micrograph. As the sample was not stained with heavy metals, only the naturally electron-dense structures were visualised; i.e., within the LL, the granular element, but not the microfibrillar matrix, was observed. Then the distribution of phosphorus was obtained by subtracting from the image at 155 eV (the energy loss peak corresponding to phosphorus) an image obtained from extrapolating data from slightly lower energies. The image so obtained (Fig. 3E) exactly matched that of the naturally electron-dense granules. The presence of phosphorus in the granules was confirmed by the energy loss spectra (Fig. 3B): in granule-containing regions (numbered 1, 2, and 3, Fig. 3C) the experimental curve displayed peaks at 155 eV, whereas in a granule-free region (numbered 4, Fig. 3C) the experimental curve matched the theoretical background one. The images of calcium distribution (Fig. 3F) showed that this element colocalised with phosphorus in the granules. The images obtained for oxygen and nitrogen (not shown) were less defined than those obtained for phosphorus and calcium. While nitrogen seemed to be more homogeneously distributed than the other elements studied, oxygen was concentrated in the regions where granules occurred. Nitrogen signals probably arose from N-acetylated sugars, which are abundant components of the LL glycoconjugates [Kilejian and Schwabe, 1971]. That the oxygen signal from the granules should stand out over the carbohydrate-rich matrix is probably explained by the presence of water molecules in the IP_6-Ca(II) salt; as mentioned these are not expected to be removed by the conventional dehydration procedures used in the preparation of samples for microscopy. Finally, the images obtained for the carbon distribution (not shown) showed very intense signals that excluded the zones occupied by the granules; strong carbon signals from the Epon resin most probably obscured weaker signals, especially any from $Ca_5H_2IP_6 \cdot 16H_2O$, a relatively carbon-poor compound. In summary, this first approach provided strong, albeit

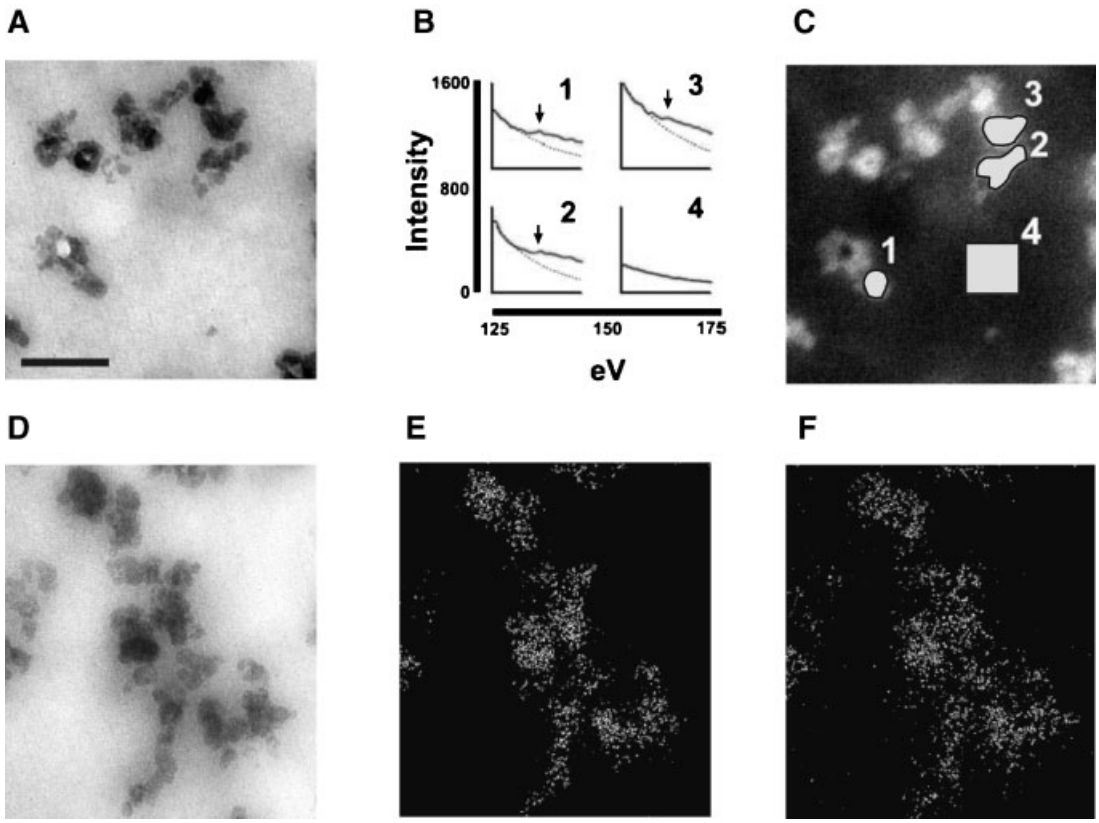

Fig. 3. Ultrastructural localisation of phosphorus and calcium in the LL by EELS. Images were obtained by EELS from unstained sections of a murine HCW. **A**, **D**: Images obtained at 0 eV (i.e. conventional transmission electron micrograph). **B**: Electron energy loss spectra (solid lines) for energy values spanning the phosphorus peak, for the selected areas shown in (**C**) (numbered 1–4); the dotted lines denote the spectral background, while arrows indicated the phosphorus peaks. **E**: Map of the phosphorus distribution; image obtained from signals arising at 120, 130, and 155 eV. **F**: Map of the calcium distribution; image obtained from signals arising at 300, 320, and 350 eV. Bar: 100 nm.

indirect, evidence that IP_6 and calcium were localised in the naturally electron-dense granules.

We next sought to confirm the result above by TEM of HCW subjected to the treatments previously shown to solubilise the IP_6-Ca(II) salt, i.e., chelating agents (EDTA or EGTA) or phytase. Although treatment of biological samples with chelating agents is in principle a low specificity method, when the supernatant resulting from extracting cysts with EDTA was analysed by ^{1}H-NMR, the only abundant organic molecules were IP_6 and EDTA (Fig. 4A). As mentioned, the second treatment used to remove IP_6 from the HCW was incubation with phytase. At the pH used in previous experiments (pH 2.5; Fig. 2), the molecule was removed from the HCW even in the absence of the enzyme; this is due to protonation of IP_6 leading to the solubilisation of the IP_6-Ca(II) salt. When the reaction was performed at pH 5.0 and in the presence of 100–500 mM $CaCl_2$, although dephosphorylation was slightly less efficient (74 vs. 80%), the molecule was totally extracted from the HCW in the presence of phytase but not in its absence (Fig. 4B). The two treatments thus validated/optimised for selective IP_6 removal were applied to ultrathin sections of HCW, which were then stained and observed under TEM. Both EGTA and phytase gave rise to the disappearance (total or near-total) of the granules in the LL (Fig. 5); in contrast, the microfibrillar matrix was unchanged. These observations confirmed that calcium IP_6 is the major component of the granular element of the LL. Moreover, the electron-dense granules observed within vesicles in the germinal layer (Fig. 5A, arrowheads) also disappeared after removal of IP_6 (Fig. 5B, arrowheads), lending additional support to the conclusion by Richards et al. [1983] that these are the same structures observed in the LL. In our hands, the size of the electron-dense

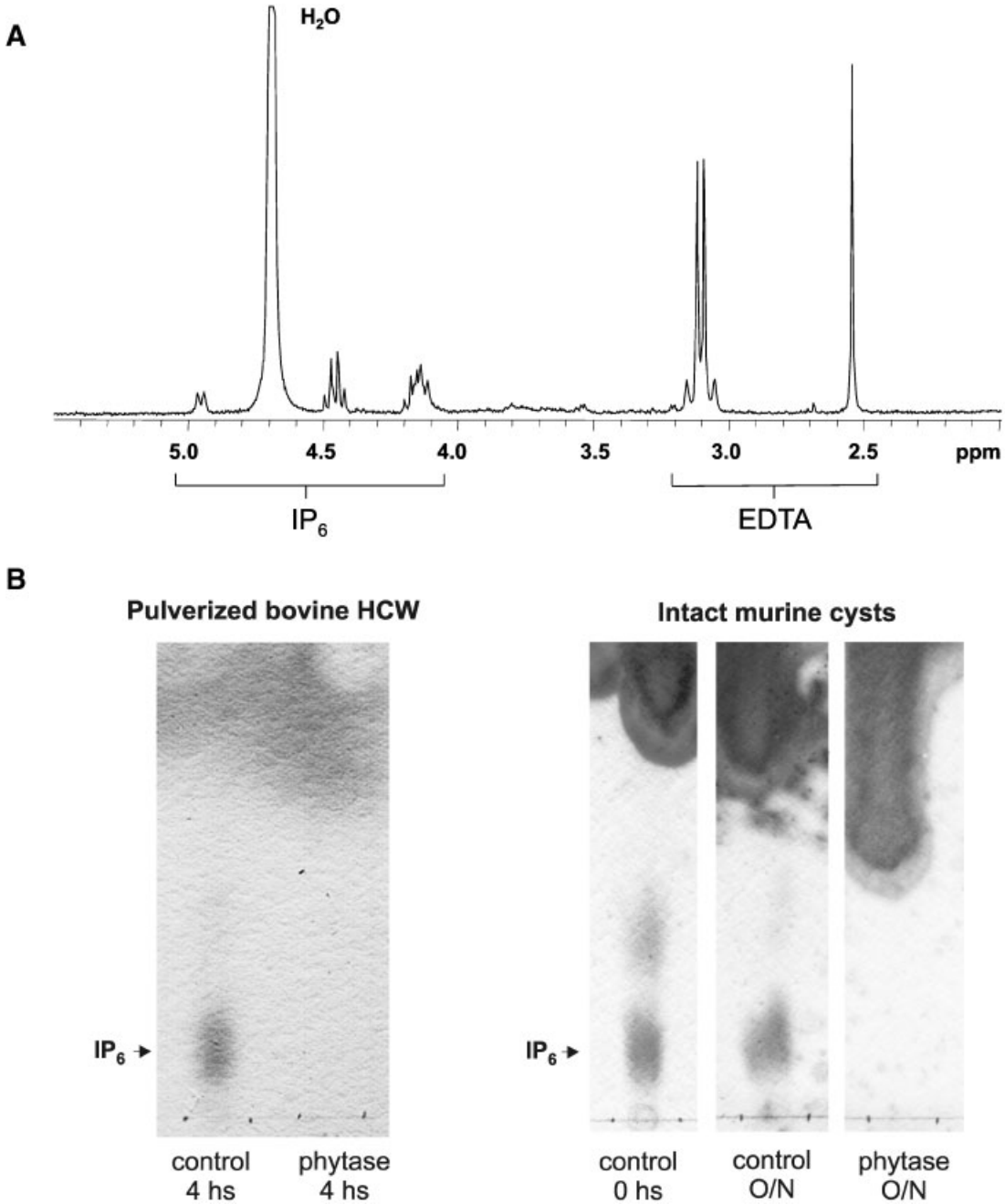

Fig. 4. Validation of the treatments employed to remove IP_6 from the HCW selectively. IP_6 was solubilised from HCW by extraction with chelating agents or dephosphorylation catalysed by phytase. **A**: ^{1}H-NMR spectrum of the EDTA extract of murine hydatid cysts. Intact cysts were incubated at 25°C for 3 h with 0.3 ml per cyst of 20 mM Tris/HCl buffer (pH 7.0) containing 5 mM EDTA. The supernatant was extensively dialysed against distilled water using a 3,500 Da cut off membrane, freeze-dried and redissolved in ^2H_2O for ^{1}H-NMR spectroscopy. The principal signals were assigned to IP_6, EDTA, and H_2O. **B**: Assessment of the level of IP_6 remaining in the HCW after dephosphorylation with phytase at pH 5.0. Pulverised bovine HCW or intact murine cysts were incubated with phytase as described in Materials and Methods for the times indicated. As a control, the samples were incubated in buffer in the absence of enzyme. Supernatants were removed and the remaining materials were washed and then incubated with EDTA-containing buffer in order to solubilise the remaining IP_6. The extracts obtained were dialysed against distilled water and a fraction thereof (equivalent to the extraction of 0.2 mg of bovine HCW dry mass or two murine cysts), were analysed by TLC on PEI-cellulose plates.

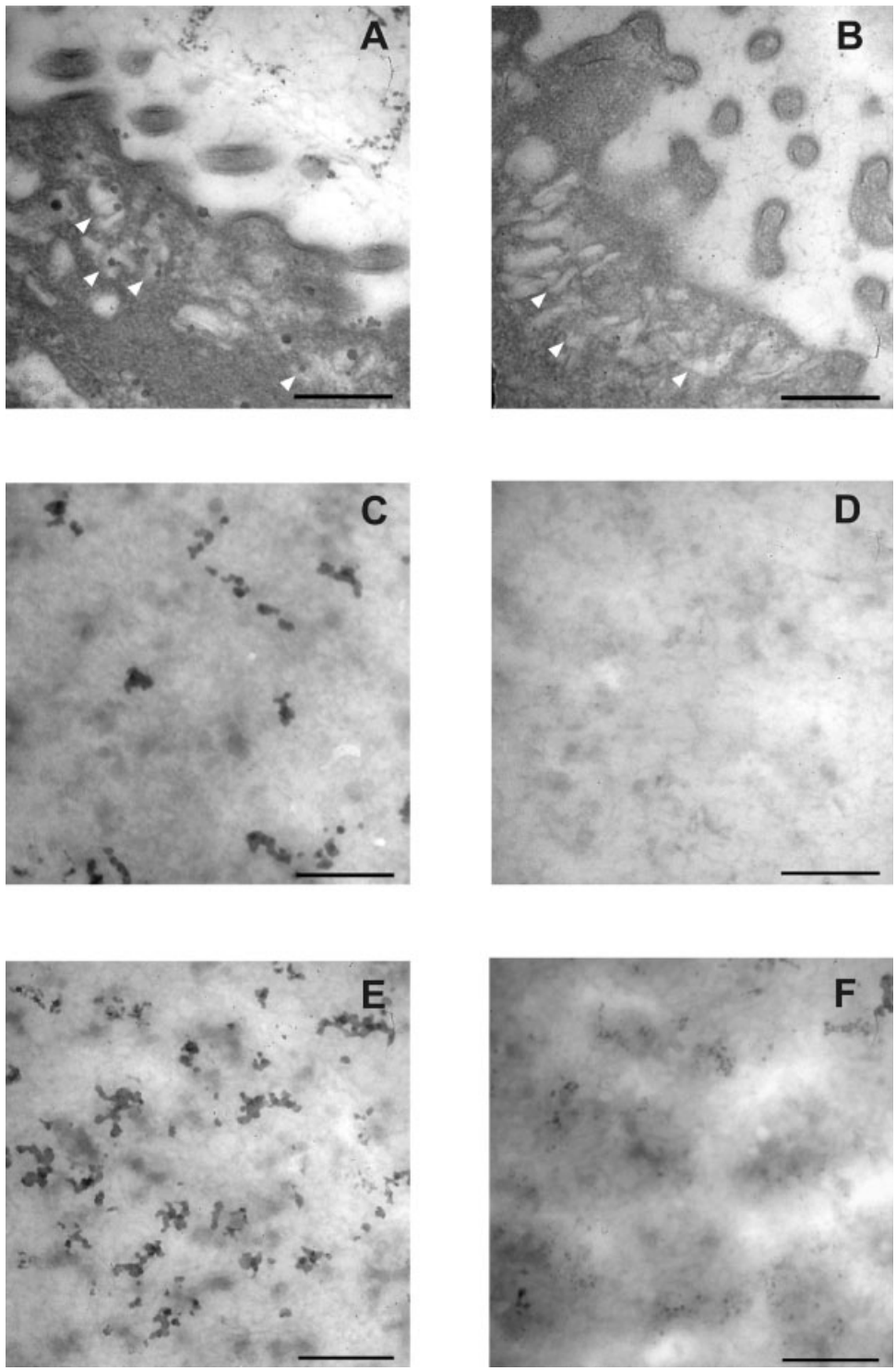

Fig. 5. Analysis of IP_6-depleted HCW by TEM. Grids containing 50-nm sections of a murine HCW were treated with EGTA or phytase so as to remove IP_6. For each treatment, a control grid was incubated under the same conditions but in the absence of chelating agent or enzyme; details of both treatments are given in the Materials and Methods section. Grids were then washed, stained with heavy metals, and analysed by TEM at 80 keV. **A** and **C**: Control of the EGTA treatment. **B** and **D**: EGTA-treated HCW **E**: Control of the phytase treatment. **F**: Phytase-treated HCW. In (A) and (B) the interface of the germinal layer and the LL is shown: note that the granules contained in vesicles in the germinal layer cells (A, arrowheads) disappear after the EGTA treatment (B, arrowheads). In parts (C) to (F) only the LL is shown. Bars: 500 nm.

granules ranged from 20 to 80 nm in diameter, with those present in the germinal layer and in the distal portion of the LL appearing larger than those present in the LL region adjacent to the germinal layer. This apparent heterogeneity is in contrast with the observation by Richards et al. [1983], that the granules had a defined size of 41 ± 1 nm in diameter; IP_6 deposits can be difficult to preserve in electron microscopy sections [Otegui et al., 2002], and we cannot rule out that the size heterogeneity arises artefactually.

Macroscopic Observations are Consistent With the Calcium-IP_6 Granules Being a Solid Phase Scattered in a gel

When intact cysts were treated with chelating agents, under conditions known to remove extracellular IP_6 selectively, the normally opaque LL became transparent (Fig. 6). This observation is consistent with the LL being made up of two different physical phases, one of which is removed by treatment with chelating agents: physically heterogeneous matter scatters light while that formed by a single phase does not. The LL can thus be envisaged as a gel, made up of highly hydrated glycoconjugates, within which solid deposits of the calcium salt of IP_6 are embedded.

DISCUSSION

The present work establishes that extracellular IP_6 in the *E. granulosus* HCW is present as its solid calcium salt, giving rise to structures previously described as naturally electron-dense granules tens of nanometers in size; this confirms the hypothesis that we had put forward in a previous communication [Irigoín et al., 2002]. The granules seem to be formed almost exclusively by the IP_6-Ca(II) salt; attempts to detect further components (as the analysis in Fig. 3A) have indicated that if they exist, they are much less abundant than the IP_6-Ca(II) salt.

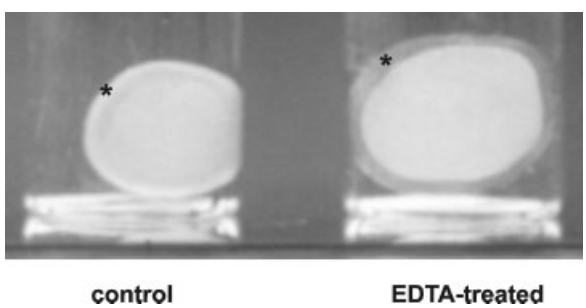

Fig. 6. Macroscopic appearance of murine cysts depleted of IP_6. Intact cysts were incubated at 25°C for 3 h with PBS containing 5 mM EDTA for IP_6 removal, or PBS alone as a control. Note that the LL (indicated by *) becomes transparent after the removal of the IP_6-Ca(II) salt. The opaque spherical shell underlying the LL is the (cellular) germinal layer.

Richards et al. [1983a] had described that granules apparently identical to the ones in the LL were present inside vesicles in the germinal layer cells. Our observation that a treatment removing IP_6 selectively from the HCW led to the disappearance of the granules present both in the LL and within cells confirms that the two are the same structure. Thus, IP_6 synthesised in germinal layer cells precipitates with calcium within a vesicular compartment, and is then exocytosed, in a polarised fashion, towards the LL. This situation has parallels with what it is observed in plant seeds, in which IP_6 is present inside membrane vesicles (vacuoles) or the endoplasmic reticulum (ER) as salts of different metal cations [Otegui et al., 2002]; in plants, however, the salts, thought to constitute a storage of phosphorus and minerals, are not secreted. The cellular distribution of IP_6 in plant cells suggest the existence of a transporter for IP_6 or a precursor across internal membranes [Otegui et al., 2002]. In animal cells, an IP_6 transporter in the ER membranes has been suggested in order to explain that the only enzyme known to dephosphorylate IP_6, the multiple inositol polyphosphate phosphatase, present exclusively in the ER, is able to modify the cytosolic levels of IP_6 [Chi et al., 2000]. Our results call for a similar transporter (in ER or another vesicular transport system membrane) in *E. granulosus*.

The function of the deposits of calcium-IP_6 in the biology of the *E. granulosus* larva is still an open question. Several facts should be borne in mind when considering this problem. First, we are dealing with a very abundant component; the figures obtained in this work indicate that IP_6-Ca(II) salt accounts for over a third of the dry mass of HCW from bovine-derived (thus large, years-old) cysts. Thus a structural role is an obvious hypothesis. In fact, EDTA-treated HCW could not be fine-sectioned for microscopy, the LL collapsing in the process; however, structural calcium not associated with IP_6 may well exist in the LL. Second, the presence of abundant calcium-IP_6 is a characteristic of the *E. granulosus* LL not shared with other members of the genus: at the ultrastructural level,

the LL of other *Echinococcus* species do not display the electron dense granules [Ingold et al., 2000, 2001], and moreover, IP_6 was not detected chemically in the HCW of *E. multilocularis* [Irigoín et al., 2002]. It is possible to envisage a function for IP_6 related to characteristics that are unique of *E. granulosus*. The ability of *E. granulosus* larva to control host inflammation is remarkable and stands in contrast to the situation seen in (the much more invasive) *E. multilocularis*. Histological studies show that inflammatory cells around the *E. granulosus* cysts can phagocytose the IP_6-Ca(II) deposits ([Richards et al., 1983b] and our own observations). The consequences upon cell function and viability of this ingestion, and their eventual relation to host inflammation control, will be the subject of further investigations.

ACKNOWLEDGMENTS

The authors thank Dr. Gabriel Cavalli (Facultad de Química, Universidad de la República, Uruguay) and Dr. Andrew Hemphill (Institute of Parasitology, University of Berne, Switzerland) for helpful discussions and suggestions, Dr. Carlos Kremer for sound advice on IP_6 chemistry, Dr. Ana Ferreira (Cátedra de Inmunología, Facultad de Química/Ciencias, Universidad de la República, Uruguay) for the fixation of the murine material for TEM, and Margarita González (Cátedra de Inmunología, Facultad de Química/Ciencias, Uruguay) for technical assistance. This work was funded by the Comisión Sectorial de Investigación Científica (CSIC, Uruguay) through grants to AD and A. M. Ferreira (2000–2002) and to AD (2002–2004), Programa para el Desarrollo de las Ciencias Básicas (PEDECIBA, Uruguay) through a scholarship to FI, and Wellcome Trust through a Research and Development Award in Tropical Medicine to AD.

REFERENCES

Bortoletti G, Ferretti G. 1978. Ultrastructural aspects of fertile and sterile cysts of *Echinococcus granulosus* developed in hosts of different species. Int J Parasitol 8: 421–431.

Chen PS, Toribara TY, Warner H. 1956. Microdetermination of phosphorous. Analytical Chem 28:1756–1761.

Chi H, Yang X, Kingsley PD, O'Keefe RJ, Puzas JE, Rosier RN, Shears SB, Reynolds PR. 2000. Targeted deletion of Minpp1 provides new insight into the activity of multiple inositol polyphosphate phosphatase in vivo. Mol Cell Biol 20:6496–6507.

Ingold K, Gottstein B, Hemphill A. 2000. High molecular mass glycans are major structural elements associated with the laminated layer of in vitro cultivated *Echinococcus multilocularis* metacestodes. Int J Parasitol 30: 207–214.

Ingold K, Dai W, Rausch RL, Gottstein B, Hemphill A. 2001. Characterization of the laminated layer of in vitro cultivated *Echinococcus vogeli* metacestodes. J Parasitol 87:55–64.

Irigoín F, Ferreira F, Fernández C, Sim RB, Díaz A. 2002. *myo*-Inositol hexakisphosphate is a major component of an extracellular structure in the parasitic cestode *Echinococcus granulosus*. Biochem J 362:297–304.

Irvine RF, Schell MJ. 2001. Back in the water: The return of the inositol phosphates. Nat Rev Mol Cell Biol 2: 327–338.

Kilejian A, Schwabe CW. 1971. Studies on the polysaccharides of the *Echinococcus granulosus* cyst, with observations on a possible mechanism for laminated membrane formation. Comp Biochem Physiol B 40:25–36.

Kilejian A, Sauer K, Schwabe C. 1962. Host–parasite relationship in *Echinococcosis*. VIII. Infrared spectra and chemical composition of the hydatid cyst. Exp Parasitol 12:377–392.

Morseth DJ. 1967. Fine structure of the hydatid cyst and protoscolex of *Echinococcus granulosus*. J Parasitol 53: 312–325.

Otegui MS, Capp R, Staehelin LA. 2002. Developing seeds of Arabidopsis store different minerals in two types of vacuoles and in the endoplasmic reticulum. Plant Cell 14:1311–1327.

Raboy V. 2003. *myo*-Inositol-1,2,3,4,5,6-hexakisphosphate. Phytochemistry 64:1033–1043.

Richards KS, Arme C, Bridges JF. 1983a. *Echinococcus granulosus equinus*: An ultrastructural study of the laminated layer, including changes on incubating cysts in various media. Parasitology 86:399–405.

Richards KS, Arme C, Bridges JF. 1983b. *Echinococcus granulosus equinus*: An ultrastructural study of murine tissue response to hydatid cysts. Parasitology 86:407–417.

Rogan MT, Richards KS. 1989. Development of the tegument of *Echinococcus granulosus* (Cestoda) protoscoleces during cystic differentiation in vivo. Parasitol Res 75:299–306.

Sadanand AV. 1971. Biochemical analyses of the cyst wall of *Echinococcus granulosus* Batsch. Comp Biochem Physiol B 40:797–805.

Shears SB. 2001. Assessing the omnipotence of inositol hexakisphosphate. Cell Signal 13:151–158.

Spencer CL, Stephens LR, Irvine RF. 1990. Separation of higher inositol phosphates by polyethileneimine-cellulose thin layer chromatography and by Dowex chloride column chromatography. In: Irvine RF, editor. Methods in inositide research. New York: Raven Press, p 40.

Van der Kaay J, Van Haastert PJ. 1995. Desalting inositol polyphosphates by dialysis. Anal Biochem 225:183–185.